

Polarization degrees-of-freedom in electronuclear hadron production from finite nuclei

J. Ryckebusch *, D. Debruyne and W. Van Nespen

Department of Subatomic - and Radiation Physics, University of Gent, Proeftuinstraat 86, B-9000 Gent, Belgium

Abstract. The polarization degrees-of-freedom in electronuclear two-nucleon knockout reactions are discussed. Model calculations for the unpolarized $^{16}\text{O}(\text{e},\text{e}'\text{pp})$ cross sections at $(|\mathbf{q}|, \omega) = (210 \text{ MeV}, 300 \text{ MeV}/c)$ are compared to recently obtained data. Predictions for the polarization observables in electronuclear two-nucleon knockout are presented. It is stressed that detailed studies of two-nucleon emission processes permit to constrain the contribution from two-nucleon mechanisms (like meson-exchange and isobar effects) to the single-nucleon knockout channel $(\text{e},\text{e}'\text{p})$.

1 Introduction

A systematic study of $(\text{e},\text{e}'\text{p})$ measurements at $x = \frac{-q^0 q_\mu}{2M_N \omega} \approx 1$ (quasi-elastic conditions) suggested a picture of the nucleus that is roughly compatible with *70% mean-field behaviour and 30% "correlations"* [1]. In such a picture, the single-particle spectral function, that determines the joint probability to remove a nucleon with momentum \mathbf{k} and to find the (bound or unbound) residual system at an excitation energy E can be formally written as [2]

$$P(\mathbf{k}, E) \equiv P_0(\mathbf{k}, E) + P_1(\mathbf{k}, E) , \quad (1)$$

where P_0 (P_1) is the mean-field ("correlations") part. The energy E is usually expressed relative to the ground-state energy of the target nucleus. The correlations part in the spectral function is generally conceived as mainly arising from two-body correlations and its strength is thought to be concentrated around a ridge determined by the following relation between the energy and momentum

$$\langle E \rangle = \frac{|\mathbf{k}|^2}{2M_N} + S_{2N} , \quad (2)$$

where S_{2N} is the threshold for two-nucleon emission out of the target nucleus. The above formulae is a formulation of a picture in which the correlations are assumed to stem from strongly correlated nucleon pairs with small c.o.m. momentum [3]. With the aid of the electromagnetic probe, access to the correlated part of the spectral function is hoped to come from semi-exclusive $(\text{e},\text{e}'\text{p})$ measurements that scan high missing-energy regions in the $A=1$ system and two-nucleon

* Talk Presented at the Workshop On Electron-Nucleus Scattering, Elba Internal Physics Center, June 22-26, 1998.

knockout measurements. With the latter technique both “correlated” partners are detected, yielding accurate information about the initial conditions of the correlated nucleon pairs. In this talk the potency of polarization degrees of freedom in probing the correlations and (possible) medium modifications in nuclei will be addressed. I will concentrate on two-nucleon knockout processes. Towards the end of the talk, however, it will be stressed that a better understanding of the two-nucleon degrees-of-freedom (d.o.f) that results from these two-nucleon knockout studies is a prerequisite for an unambiguous interpretation of ongoing and planned (e,e’p) measurements.

2 Structure functions and (polarization) observables in (e,e’NN) and (γ ,NN)

The cross section for a process in which a reaction of the type

$$A + \vec{e}(\epsilon) \longrightarrow (A-2)(E_{A-2}, \mathbf{p}_{A-2}) + N(E_1, \mathbf{p}_1) + N(E_2, \mathbf{p}_2) + e(\epsilon') \quad (3)$$

leads to the excitation of the residual nucleus A-2 in a specific state, reads

$$\begin{aligned} \frac{d^8 \sigma}{dE_1 d\Omega_1 d\Omega_2 d\epsilon' d\Omega_{\epsilon'}}(\vec{e}, e' N_1 N_2) &= \frac{1}{4(2\pi)^8} p_1 p_2 E_1 E_2 f_{rec}^{-1} \sigma_M \\ &\times \left[v_T W_T + v_L W_L + v_{LT} W_{LT} + v_{TT} W_{TT} + h \left[v'_{LT} W'_{LT} + v'_{TT} W'_{TT} \right] \right] \quad (4) \end{aligned}$$

where f_{rec} is the recoil factor and σ_M the Mott cross section. Apart from the dependence on the momentum and energy transfer (\mathbf{q}, ω) from the electrons, all structure functions W exhibit an explicit dependence on the variables ($p_1, p_2, \theta_1, \theta_2$ and $\phi_1 - \phi_2$) characterizing the momentum and spatial direction of the two escaping nucleons. In addition, the W_{LT} , W_{TT} and W'_{LT} structure functions depend on the azimuthal angle of the center-of-mass $\frac{\phi_1 + \phi_2}{2}$ that can be pulled out of the structure functions.

We remind that apart from a negligible parity-violating component, the structure function $W'_{LT}=0$ in coplanar kinematics and W'_{TT} vanishes identically, independent of the kinematics. More favorable situations are created when performing polarimetry on one of the ejected hadrons and the spin projection of the latter can be determined. In what follows, the polarization of the escaping nucleon is expressed in the reference frame determined by the unit vectors (Fig. 1)

$$\hat{\mathbf{l}} = \frac{\mathbf{p}_1}{|\mathbf{p}_1|} \quad \hat{\mathbf{n}} = \frac{\mathbf{q} \times \mathbf{p}_1}{|\mathbf{q} \times \mathbf{p}_1|} \quad \hat{\mathbf{t}} = \hat{\mathbf{n}} \times \hat{\mathbf{l}}. \quad (5)$$

The escaping nucleon polarization observables can be determined through measuring **ratios**

$$\begin{aligned} P_i &= \frac{\sigma(s_{1i} \uparrow) - \sigma(s_{1i} \downarrow)}{\sigma(s_{1i} \uparrow) + \sigma(s_{1i} \downarrow)} \\ P'_i &= \frac{[\sigma(h=1, s_{1i} \uparrow) - \sigma(h=-1, s_{1i} \uparrow)] - [\sigma(h=1, s_{1i} \downarrow) - \sigma(h=-1, s_{1i} \downarrow)]}{[\sigma(h=1, s_{1i} \uparrow) + \sigma(h=-1, s_{1i} \uparrow)] + [\sigma(h=1, s_{1i} \downarrow) + \sigma(h=-1, s_{1i} \downarrow)]} \end{aligned}$$

where $s_{1i} \uparrow$ denotes that hadron “1” is spin-polarized in the positive i direction ($i=(n,l,t)$) and h is the helicity of the electron impinging on the target nucleus.

For the sake of completeness we mention that for real photons, the unpolarized differential cross section and asymmetry reads in terms of the structure functions as

$$\frac{d^6\sigma}{d\Omega_1 d\Omega_2 dE_1 dE_2} = \frac{1}{(2\pi)^5 2E_\gamma} p_1 p_2 E_1 E_2 \delta(E_{A-2} + E_1 + E_2 - E_A - E_\gamma) \frac{1}{2} W_T$$

$$\Sigma = \frac{d\sigma_{\parallel}(\gamma, NN) - d\sigma_{\perp}(\gamma, NN)}{d\sigma_{\parallel}(\gamma, NN) + d\sigma_{\perp}(\gamma, NN)} = -\frac{W_{TT}}{W_T}, \quad (6)$$

where \parallel (\perp) denotes that the photon is polarized parallel (perpendicular) to the reaction plane determined by the photon and one of the ejected nucleon's momentum.

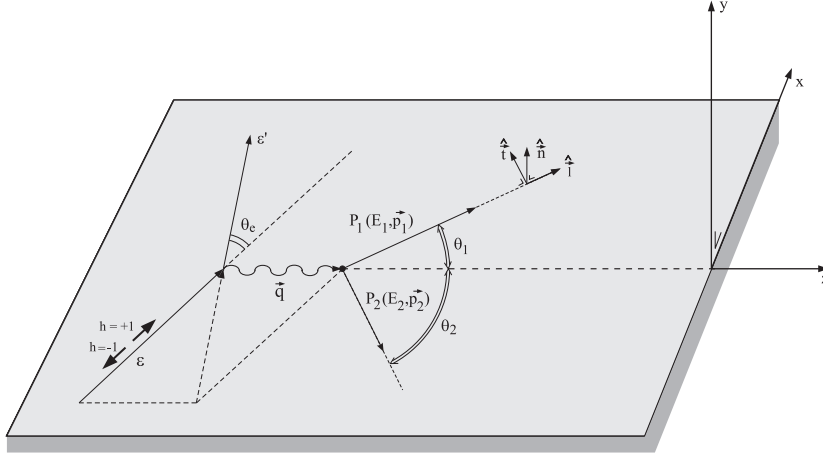


Fig. 1. Reference frame in which the nucleon polarization for the $(\vec{e}, e' \vec{N} \dots)$ reaction is determined. A coplanar situation is considered.

3 A model for two-nucleon photoproduction on nuclei

Dealing with both the unpolarized and polarized observables it is advantageous to calculate the transition matrix elements in the helicity basis

$$m_F^{fi}(\lambda = \pm 1, 0) = \left\langle \Psi_f^{A-2}(E_x, J_R M_R); \mathbf{p}_1 m_{s_1} \mathbf{p}_2 m_{s_2} \mid J_{\lambda=\pm 1, 0}(\mathbf{q}) \mid \Psi_0 \right\rangle, \quad (7)$$

where Ψ_0 is the ground state of the target system, $\Psi_f^{A-2}(E_x, J_R M_R)$ the (discrete or continuum) state in which the final nucleus is created and $(\mathbf{p}_1 m_{s_1} \mathbf{p}_2 m_{s_2})$

the asymptotic momenta and spin projections (along the z-axis which coincides with the direction of the momentum transfer) of the ejected particles. The basic assumptions of the model that is used to calculate the (e,e'NN) and (γ ,NN) cross sections are summarized below. More details can be found in Refs. [4, 5, 6].

- A consistent shell-model description for the initial and final state is adopted. In this manner, orthogonality and anti-symmetry conditions are naturally obeyed. Moreover, the calculations for the $A(\gamma,pp)$ and $A(e,e'pp)$ reaction channels, to which charged pion exchange is not contributing, are GAUGE INVARIANT.
- A distorted wave description for the ejectiles is adopted.
- The spectator approximation is adopted. This implies that only two nucleons are considered to be directly involved in the reaction process. The remaining $A-2$ nucleons are behaving as spectators. This assumption does restrict the applicability of the model calculations to the energy region just above the two-nucleon emission threshold for which the exclusive character of the reaction can be guaranteed and there is ample of empirical evidence that the reaction proceeds in a direct knockout manner.
- The cross sections are calculated for each individual state in the $A-2$ system.
- In the model, the center-of-mass and relative motion of the pair is treated in its full complexity. We start from a realistic set of single-particle wave functions obtained from a Hartree-Fock calculation. With these single-particle wave functions a satisfactory description of the quasi-elastic (e,e'p) data for $A \geq 12$ could be obtained [7]. Unlike for a harmonic-oscillator basis, no formal separation into relative and c.o.m. coordinates can be pursued.
- The pionic degrees of freedom are assumed to be the carriers of the medium-range two-nucleon effects. We include the equivalent of all types of Feynman diagrams that are commonly implemented in a diagrammatic description for pion photoproduction on the nucleon $\gamma + N \rightarrow N + \pi$. This includes the Seagull, pion-in-flight and those diagrams that involve a Δ_{33} resonance.
- One of the major goals of two-nucleon knockout mechanisms is to enrich our knowledge about the short-range correlations (SRC) and to test the different models that deal with these effects. In an attempt to connect the cross sections directly to the predictions of many-body theories we start with correlated wave functions of the type

$$\bar{\Psi} = \frac{\hat{G}\Psi}{\langle \Psi | \hat{G}^\dagger \hat{G} | \Psi \rangle}, \quad (8)$$

where the operator \hat{G} accounts for the corrections on the Slater determinants

$|\Psi\rangle$

$$\hat{\mathcal{G}} = \hat{\mathcal{S}} \prod_{i < j=1}^A \sum_p f^p(\mathbf{r}_{ij}, \mathbf{R}_{ij}) \hat{O}^{[p]}, \quad (9)$$

where $\hat{\mathcal{S}}$ is the symmetrizing operator and p usually runs over a variety of operators. The correlated wave function of Eq. (8) contains 2,3,...,A-body correlations. In the calculations, the two-body terms in the first-order cluster expansion of the transition matrix elements (7) are retained. This approach is justified by remarking that a recent first-order cluster calculation of the two-nucleon knockout contribution to the longitudinal $^{12}\text{C}(e,e')$ strength illustrated that the two-body terms account for the major effect of the central short-range correlations [8]. In our calculations, the correlation functions $f^p(\mathbf{r}_{ij})$ are taken from many-body theories. The reaction model calculations of which some selective results will be presented further on should be regarded upon as the link between the predictions of many-body theories and the actual data. It is generally accepted that the (e,e'pp) cross sections are primarily sensitive to the central part in the correlation operator

$$\hat{\mathcal{G}} = \hat{\mathcal{S}} \prod_{i < j=1}^A f^C(\mathbf{r}_{ij}) \hat{1}, \quad (10)$$

that finds its origin in the hard-core repulsion at short internucleon distances.

4 Results and discussion

4.1 The $^{16}\text{O}(e,e'\text{pp})$ reaction at low Q^2

Before turning to some predictions for the polarization observables in two-nucleon knockout studies, a comparison between the model predictions and some recent $^{16}\text{O}(e,e'\text{pp})$ measurements from NIKHEF [9, 10, 11] is presented. The measurements utilized hadron detectors that have a rather wide solid angle ($\Delta\theta \approx 30^\circ$). For that reason, the calculations had to be performed in a grid that covers the full polar and kinetic energy acceptance of the hadron detectors at a central value for the electron kinematics ($\omega=210$ MeV/c, $q=300$ MeV/c). In the quasi-elastic (e,e'p) case, the dominant peaks in the low-energy part of the missing energy spectrum can usually be interpreted in terms of one single-hole component which makes the nuclear-structure input in the calculations rather simple. In the two-nucleon knockout case, however, an additional complication in the calculations stems from the fact that nuclear-structure calculations [14, 15] point towards two-body overlap wave functions between the A target and A-2 residual nucleus that can have several two-hole components with a sizeable amplitude. The sophisticated nuclear-structure calculations from Ref. [15], that were also at the basis of the theoretical analysis presented in Ref. [10] predict the following two-proton removal amplitudes for a transition from the ^{16}O ground-state to the low-lying states with predominant two-hole character in ^{14}C

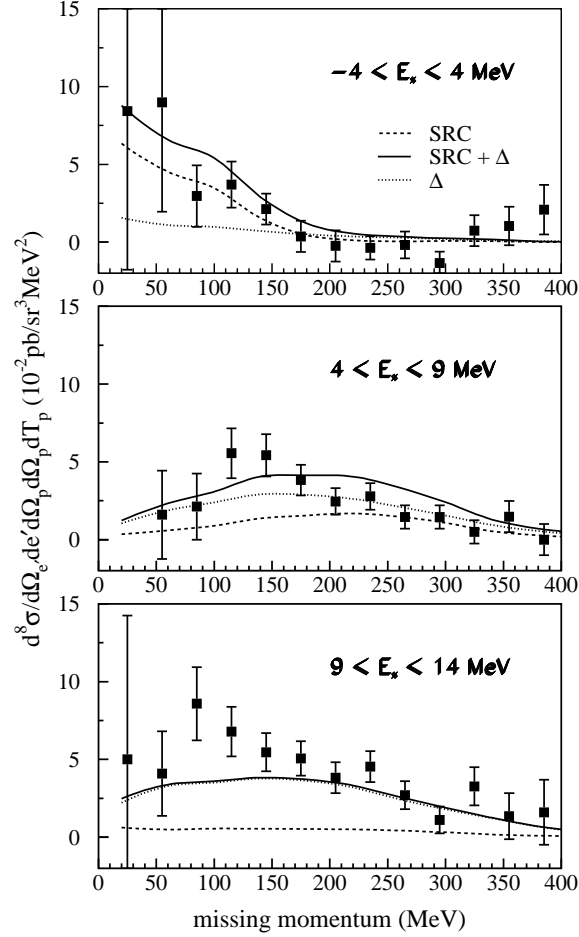
$^{16}\text{O}(e,e'pp)^{14}\text{C} ; \omega=210 \text{ MeV} ; q=300 \text{ MeV}/c$


Fig. 2. Calculated $^{16}\text{O}(e,e'pp)$ missing momentum distributions for various groups of final states and electron kinematics determined by $e=580 \text{ MeV}$, $e'=374 \text{ MeV}$ and $\theta_e=26.2^\circ$. The two-nucleon knockout phase-space covered is determined by $15^\circ \leq \theta_1 \leq 43^\circ$, $116^\circ \leq \theta_2 \leq 148^\circ$ and $52 \text{ MeV} \leq T_2 \leq 108 \text{ MeV}$. The polar angles are expressed relative to the direction of the momentum transfer. In each of these variables five mesh points were considered. The data are from Ref. [10]. The solid line is the result of the distorted-wave calculation when both the SRC and Δ isobar effects are included. The dotted (dashed) line includes solely the Δ isobar (SRC) effects.

$$\begin{aligned}
|0^+; g.s.\rangle &= 0.77 \left| (p_{1/2})^{-2}; 0^+ \right\rangle + 0.18 \left| (p_{3/2})^{-2}; 0^+ \right\rangle \\
|2^+; E_x = 7.0, 8.3 \text{ MeV} \rangle &= 0.11 \left| (p_{3/2})^{-2}; 2^+ \right\rangle - 0.77 \left| (p_{3/2})^{-1} (p_{1/2})^{-1}; 2^+ \right\rangle \\
|1^+; E_x = 11.3 \text{ MeV} \rangle &= 0.77 \left| (p_{1/2})^{-1} (p_{3/2})^{-1}; 1^+ \right\rangle .
\end{aligned} \tag{11}$$

A striking feature of these removal amplitudes is their smallness. They are compatible with single-nucleon spectroscopic factors of the order $\frac{S_{lj}}{(2j+1)} \approx 0.7$ that were systematically obtained in the analysis of quasi-elastic (e,e'p) measurements [1]. Indeed, the two-nucleon spectroscopic factors corresponding with the above removal amplitudes are

$$\frac{S_{lj,l'j'}}{(2j+1)(2j'+1)} \approx 0.5 , \tag{12}$$

which is approximately equal to the values that one would obtain by relying on a rather crude estimate based on

$$\frac{S_{lj,l'j'}}{(2j+1)(2j'+1)} \approx \frac{S_{lj}}{(2j+1)} \frac{S_{l'j'}}{(2j'+1)} , \tag{13}$$

and putting $\frac{S_{lj}}{2j+1} \approx 0.7$ as the quasi-elastic (e,e'p) measurements seem to suggest. Recent $^{16}\text{O}(\text{e,e'pp})$ measurements at the MAMI facility with superior energy resolution [12] point towards a strong population of the states at $E_x=0.0, 7.0, 8.3$ and 11.3 MeV excitation energy in ^{14}C . These are exactly the ^{14}C states that were observed to be strongly populated in a $^{15}\text{N}(\text{d},^3\text{He})$ pick-up experiment [13] which points towards their strong two-hole character relative to the ground-state of ^{16}O . In comparison with the two-nucleon overlap wave functions as they were derived by Cohen and Kurath [14], the wave functions of Eq. (11) are characterized by smaller amplitudes and a weaker mixing between the $\left| (p_{1/2})^{-2} \right\rangle$ and the $\left| (p_{3/2})^{-2} \right\rangle$ configurations for the ground-state to ground-state transition. The results presented below are obtained with the above wave functions, an exception made for the fact that for the ground-state to ground-state transition we adopt the relative mixing between the two configurations as it was predicted by Cohen and Kurath. In practice, this amounts to replacing the amplitude 0.18 in the first line of Eq. (11) by 0.31. This operation is inspired by the observation that with this wave function a more favorable agreement between the model calculations and the high-resolution data from Mainz is reached [12].

The results of the calculations for the three lowest bins in the excitation energy spectrum obtained from the NIKHEF experiment are shown in Figure 2. The comparison between the calculations and the data is done as a function of the pair missing momentum

$$|\mathbf{P}| = |\mathbf{p}_1 + \mathbf{p}_2 - \mathbf{q}| . \tag{14}$$

Despite the fact that the experimental resolution in the excitation (or missing) energy was of the order of 4 MeV and the individual states could strictly not be resolved, the above considerations allow to infer that the lowest excitation-energy bin ($-4 \text{ MeV} \leq E_x \leq 4 \text{ MeV}$) is as good as exclusively fed through the ^{14}C ground-state transition, whereas the second and third bin are mainly fed through the $|2^+; E_x = 7.01, 8.32 \text{ MeV}\rangle$ and the $|1^+; E_x = 11.3 \text{ MeV}\rangle$ states. The overall agreement between the calculations and the data is satisfactory. In line with the conclusions reached in Ref. [16], a striking feature of the “SRC” contribution is that it is significantly more important for the ground-state transition in comparison with the other two transitions. This feature can be explained as follows. First, within a harmonic oscillator basis the sole contributions to the $^{16}\text{O}(0^+, \text{g.s.}) + e \rightarrow e' + p + p + ^{14}\text{C}(0^+, \text{g.s.})$ process stems from the $^1S_0(T=1)$ and $^3P_1(T=1)$ configurations for the relative diproton wave function. As the 3P_1 configuration necessarily implies a c.o.m. P-wave the low missing part of the ground-state transition is a clear signal of the $^1S_0(T=1)$ configuration. Therefore it is expected to be very sensitive to the short-range correlations, a property which is confirmed by the calculations. Second, it turns out that the Δ contribution is strongly suppressed for the $A(0^+) \rightarrow A-2(0^+)$ transition. In an attempt to explain this observation we remark that within the context of $(\vec{\gamma}, pp)$ reactions it was shown that the photon asymmetry Σ equals approximately -1 as long as the initial photoabsorption can be guaranteed to occur on diprotons residing in a relative $^1S_0(T=1)$ state [17, 6]. In terms of structure functions, Eq. (6) suggests that under these conditions the W_T will be approximately equal to W_{TT} . At the cross section level this implies that as long as the initial photoabsorption occurs on a $^1S_0(T=1)$ diproton and the final state interaction has a similar impact on the W_T and W_{TT} structure functions one has

$$v_T W_T + v_{TT} W_{TT} \approx \tan^2 \frac{\theta_e}{2} W_T \quad (15)$$

suggesting that the Δ isobar currents, which represent the major contribution to the transverse channel, will decrease in importance as smaller electron angles are probed. A similar sort of cancellation between the W_T and W_{TT} terms, though an exact one, was noted for the coherent $A(0^+, \text{g.s.}) + e \rightarrow A(0^+, \text{g.s.}) + e' + \pi^0$ reaction [18].

4.2 (e,e'pp) reactions in super-parallel kinematics

We now turn to the polarization observables in two-proton knockout and concentrate on one specific kinematics situation which is judged favorable for these studies. So-called super-parallel kinematics corresponds with the situation that both nucleons are ejected along the direction of the momentum transfer. Recent $^{12}\text{C}(e, e' p \pi^-)$ calculations illustrate that resonant pion production peaks for $\theta_\pi \approx 90^\circ$ [20]. For that reason, Δ isobar contributions to $(e, e' pp)$ that are originating from initial resonant pion production with subsequent reabsorption are expected to reach a maximum for both nucleons moving perpendicular to

the direction of the momentum transfer and to be suppressed in super-parallel kinematics. Given the large amount of independent variables that determine the two-nucleon knockout cross sections, an obvious and probably more interesting asset of super-parallel kinematics is that only a selected number of structure functions will contribute to the (e,e'pp) cross section and polarization observables [21]. It is to be expected that this property will facilitate the interpretation of the data. The selectivity of the cross section and polarization observables to the different structure functions for planar (e,e'pp) processes in super-parallel kinematics is illustrated in Table 1. Theoretical predictions within the model outlined in Section 3 are shown in Figure 3. We have selected the kinematics of the approved MAMI experiment A1/1-97 [22].

Table 1. *The structure functions determining the cross section (c.s.) and polarization observables for planar $(\vec{e}, e' \vec{p} p)$ reactions in super-parallel kinematics*

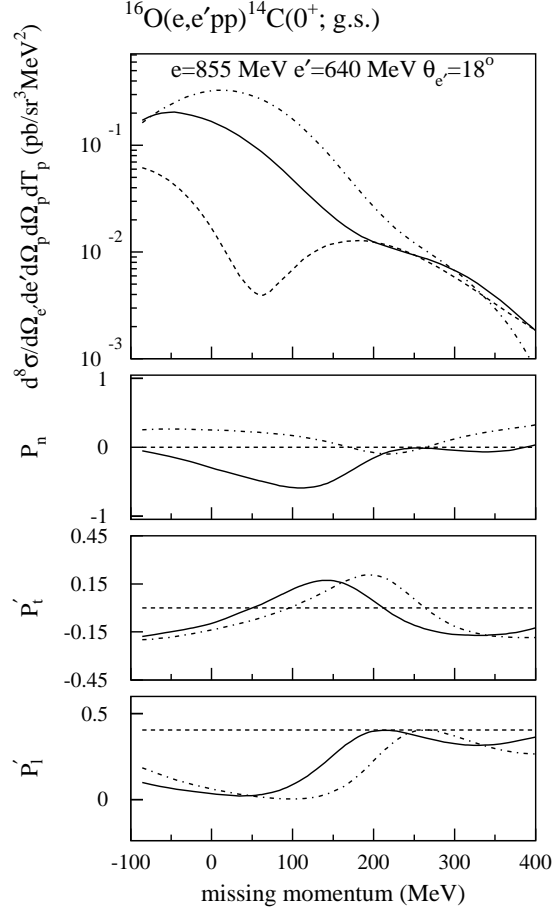
c.s.	W_L, W_T	(e,e'pp)
P_n	W_{LT}	(e,e' $\vec{p} p$)
P'_l	W'_{TT}	($\vec{e}, e' \vec{p} p$)
P'_t	W'_{LT}	($\vec{e}, e' \vec{p} p$)

From Figure 3 it is clear that the central short-range correlations dominate the ground-state transition up to pair missing momenta of about 150 MeV/c which is in line with the results obtained in Section 4.1 (upper panel of Figure 2). Very clear signals of the central short-range correlations can be deduced from the polarization observables P_n and P'_t . Referring to Table 1 these observables reflect the interference between the longitudinal and transverse response. In the absence of central short-range correlations that feed the longitudinal channel these observables vanish identically. The presence of central correlations makes the P_n and P'_t sizeable, particularly for the low missing momentum region where their contribution is large. Remark further that the effect of the final-state interaction is substantially smaller for the double polarization observables (P'_l and P'_t) than for the differential cross section and P_n .

4.3 Multi-nucleon degrees of freedom and $(\vec{e}, e' \vec{p})$ reactions

Accumulated information about the two-hadron degrees of freedom in the nucleus that is gained from two-nucleon knockout studies with real and virtual photons will be of great value in TJNAF and MAMI(-C) (e,e'p) studies. Indeed,

Fig. 3. The missing momentum dependence of the $^{16}\text{O}(e,e'pp)^{14}\text{C}(0^+, \text{g.s.})$ differential cross section and polarization observables in super-parallel kinematics for typical MAMI kinematics. The solid curve is calculated in the distorted-wave approximation including the Δ -current and ground-state correlations. The latter are implemented through the central correlation function $f^C(r_{12})$ from the G -matrix calculation of Ref. [19]. The dot-dashed curve is the equivalent of the solid line but is calculated with plane wave outgoing nucleon waves. The dashed line is the result of a distorted-wave calculation including only the Δ current.



in many cases $\text{A}(e,e'p)$ reactions are meant to provide detailed information about single-nucleon degrees of freedom and accordingly, meson-exchange and isobaric currents are unwanted “background” that ought to be “theoretically” controlled. A few examples of $(e,e'p)$ investigations that fall into this category are

1. The $(e,e'p)$ studies at high (E_m, p_m) , which aim at probing the “correlated” part of the spectral function [23]. Major complications in the interpretation of these data in terms of the single-particle spectral function is the effect of

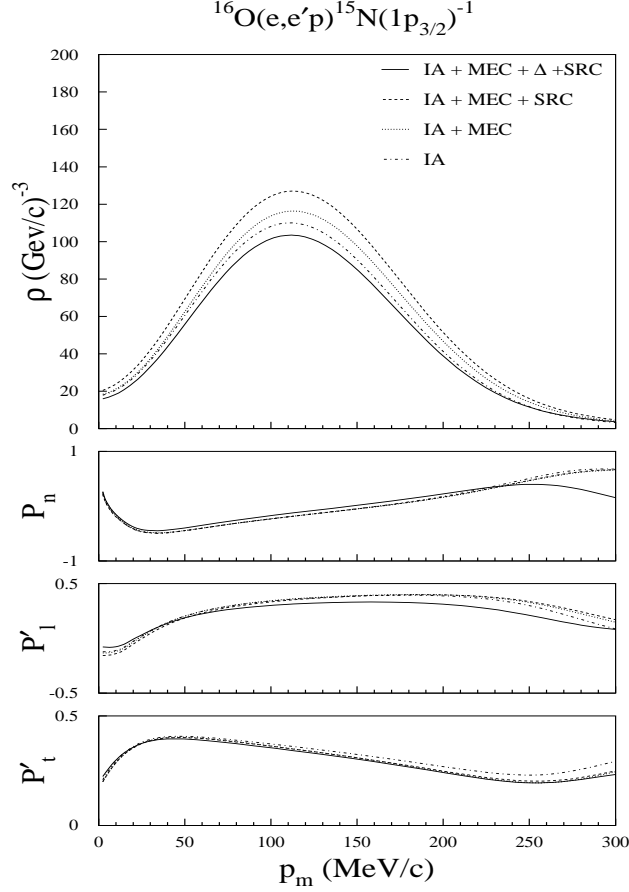


Fig. 4. The sensitivity of the distorted missing momentum distribution and polarization observables to the various two-nucleon effects. Calculations are performed for $p_{3/2}$ knockout from ^{16}O at $e=850\text{ MeV}$, $e'=610\text{ MeV}$ and $q=690\text{ MeV}/c$ ($Q^2=0.42\text{ (GeV}/c)^2$, $x=0.938$). The variation in missing momentum is reached by varying the polar angle of the ejected proton (quasi-perpendicular kinematics).

multi-step processes and multi-body current contributions [11].

2. A promising way of testing models that predict substantial medium modifications [24] for the electromagnetic form factors of the nucleon is high-precision ($\vec{e}, e' \vec{p}$) studies at moderate and high Q^2 [25]. Indeed, in the plane-wave impulse approximation (PWIA) it can be shown that

$$\frac{P'_l}{P'_t} = -\frac{G_M^p}{G_E^p} \frac{(e + e') \tan \frac{\theta_e}{2}}{2M_p}. \quad (16)$$

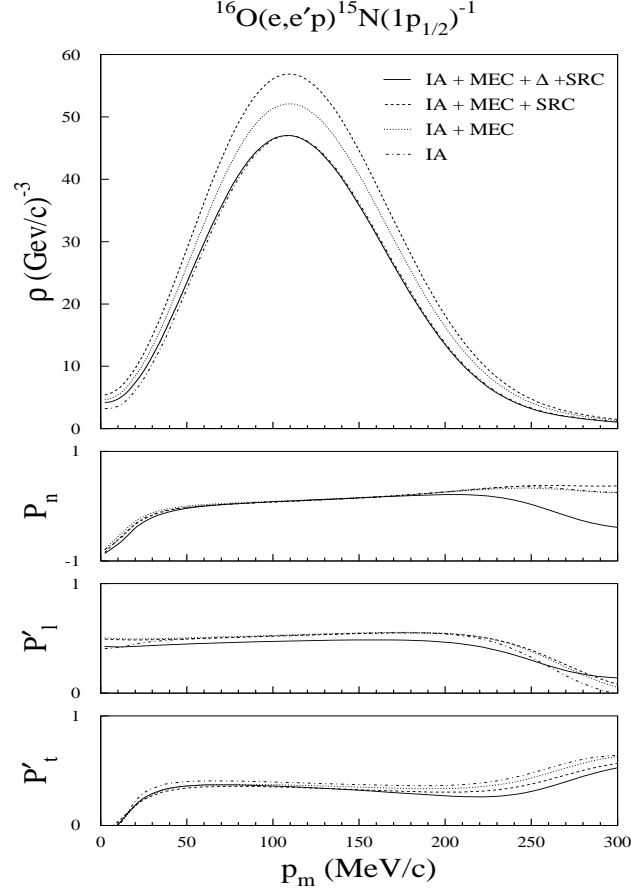


Fig. 5. As in Figure 4 but for knockout from the $1p_{1/2}$ orbit.

It is of the utmost importance to investigate all possible mechanisms that could bring about changes in the above ratio without being related to (possible) medium modifications of the form factors. Whereas it was recently shown that final-state interaction and gauge ambiguities effects are only marginally affecting the ratio $\frac{P'_l}{P'_t}$ [26] the question arises whether meson-exchange and isobaric currents could bring about any change in the ratio of the double polarization observables. In Figures 4 and 5 we show the distorted missing momentum distribution and polarization observables P_n , P'_l and P'_t for the $^{16}\text{O}(e,e'p)$ reaction under quasi-elastic conditions. Typical kinematics for the MAMI facility in Mainz was chosen ($e=850$ MeV, $e'=610$ MeV and $q=690$ MeV/c). No spectroscopic factors were introduced which means that the calculations are normalized to full subshell occupancy. We have considered all the two-nucleon effects that

are usually included in the two-nucleon knockout calculations : meson-exchange currents (MEC), Δ -isobar currents (IC) and the effect of central short-range correlations. With respect to the short-range effects we want to stress that in Ref. [5] it was shown that in the lowest order cluster expansion the short-range effects as they are introduced through equation Eq. (8) can be implemented by considering a two-body operator of the type

$$\begin{aligned}
& - \sum_{i < j} \left[\left(\mathbf{J}^{[1]}(i) + \mathbf{J}^{[1]}(j) \right) g(\mathbf{r}_{ij}) + g^\dagger(\mathbf{r}_{ij}) \left(\mathbf{J}^{[1]}(i) + \mathbf{J}^{[1]}(j) \right) \right. \\
& \quad \left. + \mathbf{J}^{[2]}(i, j) g(\mathbf{r}_{ij}) + g^\dagger(\mathbf{r}_{ij}) \mathbf{J}^{[2]}(i, j) \right]
\end{aligned} \tag{17}$$

where $\mathbf{J}^{[1]}$ is the one-body current operator as it would be considered in the impulse approximation, $\mathbf{J}^{[2]}$ the two-body current operator including the meson-exchange (MEC) and Δ -isobar (IC) currents and $g(\mathbf{r}_{ij})$ is a shorthand notation for $1 - f^C(\mathbf{r}_{ij})$. The contribution from the two-nucleon currents to the single-proton knockout channel was calculated by explicitly summing over all occupied proton and neutron single-particle states in the target nucleus [27]. Referring to Figures 4 and 5, a striking feature is that the two-nucleon effects do not significantly alter the shape of the effective missing-momentum distributions for the low missing-momentum region. As a consequence, their effect would not be noticed when comparing IA calculations with data but would simply be “effectively” accounted for in the spectroscopic factor that is introduced to scale the calculations to the data. The net effect of the various two-nucleon effects is a reduction of the $1p_{3/2}$ cross section and almost negligible in the cross section for its spin-orbit partner $1p_{1/2}$. In line with the findings of Ref. [27] the impact of the two-nucleon effects is generally bigger for the $j = l + \frac{1}{2}$ than for the corresponding $j = l - \frac{1}{2}$ single-particle state.

The effect of the two-nucleon currents on the polarization observables is rather small in the low missing momentum region for the considered quasi-elastic kinematic conditions ($x=0.94$). On the other hand, particularly the P'_l observable is predicted to exhibit some sensitivity to the Δ -isobar currents, an effect which warrants further investigation in the light of previous discussions. With increasing Q^2 the relative importance of two-body currents is expected to decrease. In this regime, however, numerical calculations with two-body currents become very involving as a large number of multipoles in the expansions of the electromagnetic current operators is required before convergence can be reached.

5 Conclusions and Outlook

In conclusion, there is accumulating evidence that both scalar short-range correlations and Δ isobar effects from $\gamma^* pp \rightarrow \Delta^+ p \rightarrow pp\pi^0 \rightarrow pp$ contribute to the A(e,e'pp) reaction. Real photon studies with polarized photons will fine-tune the different Δ and MEC mechanisms that play a role in electronuclear hadron

production. It was shown that a reasonable description of the $^{16}\text{O}(e,e'pp)$ experimental data from NIKHEF could be obtained. These two-nucleon knockout data seem to provide some evidence for the unexpectedly “low” spectroscopic factors that were obtained from the analysis of quasi-elastic $(e,e'p)$ reactions. Moreover, it turned out that the SRC effects can be clearly separated from the Δ -isobar background at low missing “diproton” momenta in accordance with the physical picture that the correlations in the single-particle spectral function $P(\mathbf{k}, E)$ are localized along a ridge imposed by the kinematical constraints of heavy repulsion between the individual nucleons that constitute pairs. It was further shown that polarization observables as they can be obtained from $(\vec{e}, e' \vec{p}p)$ measurements offer possibilities to further isolate the longitudinal channel and to minimize at the same time the uncertainties with respect to the final state interaction. The usefulness of the improved insight into the effect of two-nucleon degrees of freedom for the electromagnetic probe was illustrated for double-polarization single-nucleon knockout studies.

Acknowledgments

This work is supported by the Fund for Scientific Research (FWO) - Flanders under contract number G.0008.95. Stimulating discussions with G. Rosner are gratefully acknowledged.

References

1. V. Phandari pande, I. Sick and P.K.A. de Witt Huberts, *Rev. Mod. Phys.* **69** (1997) 981.
2. C. Ciofi degli Atti and S. Simula, *Phys. Rev. C* **53** (1996) 1689.
3. L.L. Frankfurt and M.I. Strikman, *Phys. Rep.* **160** (1988) 236.
4. J. Ryckebusch, M. Vanderhaeghen, L. Machenil and M. Waroquier, *Nucl. Phys.* **A568** (1994) 828.
5. J. Ryckebusch, V. Van der Sluys, K. Heyde, H. Holvoet, W. Van Nespen, M. Waroquier and M. Vanderhaeghen *Nucl. Phys.* **A624** (1997) 581.
6. J. Ryckebusch, D. Debruyne and W. Van Nespen, *Phys. Rev. C* **57** (1998) 1319.
7. V. Van der Sluys, J. Ryckebusch and M. Waroquier, *Phys. Rev. C* **55** (1997) 1982.
8. Giampaolo Co' and Antonio M. Lallena, *Phys. Rev. C* **57** (1998) 145.
9. C.J.G. Onderwater *et al.*, *Phys. Rev. Lett.* **78** (1997) 4893.
10. C.J.G. Onderwater *et al.*, *Phys. Rev. Lett.* **81** (1998) 2213.
11. L. Lapikàs, contribution to this proceedings.
12. G. Rosner, contribution to this proceedings.
13. G. Kaschl, G. Mairle, H. Mackh, D. Hartwig and U. Schwinn, *Nucl. Phys.* **A178** (1971) 275.
14. S. Cohen and D. Kurath, *Nucl. Phys.* **A141** (1977) 145.
15. W.J.W. Geurts, K. Allaart, W.H. Dickhoff, H. Mütter, *Phys. Rev. C* **54** (1996) 1144.
16. G. Giusti, F.D. Pacati, K. Allaart, W. Geurts, H. Muether and W. Dickhoff, *Phys. Rev. C* **57** (1998) 1691.

17. A.M. Sandozi and W. Leidemann, Phys. Rev. C **53** (1996) 1506.
18. S. Hirenzaki, J. Nieves, E. Oset and M.J. Vicente-Vacas, Phys. Lett. **B304** (1993) 198.
19. C.C.Gearhart, PhD thesis, Washington University (St. Louis, 1994), unpublished and W. Dickhoff, private communication.
20. F.X. Lee, C. Bennhold and L.E. Wright, Phys. Rev. C **55** (1997) 318.
21. C. Giusti and F.D. Pacati, Nucl. Phys. **A535** (1991) 573.
22. MAMI experiment A1/1-97 "Investigation of Short-Range nucleon-nucleon correlations using the reaction $^{16}\text{O}(e,e'pp)^{14}\text{C}$ in superparallel kinematics" (Contact Persons J. Friedrich and G. Rosner)
23. TJNAF experiment E-97-006 "Correlated Spectral Function and the (e,e'p) reaction mechanism" (Spokesperson I. Sick)
24. D.H. Lu, A.W. Thomas, K. Tsushima, A.G. Williams and K. Saito, Phys. Lett. **B417** (1998) 217.
25. R.D. Ransome, contribution to this proceedings.
26. J.J. Kelly, Phys. Rev. C **56** (1997) 2672.
27. V. Van der Sluys, J. Ryckebusch and M. Waroquier, Phys. Rev. **C49** (1994) 2695.